

# 3D Modeling of Thin Sheets in the Discontinuous Galerkin Method for Transient Scattering Analysis

Mohamed Boubekeur<sup>1</sup>, Abelin Kameni<sup>1</sup>, Laurent Bernard<sup>1</sup>, Axel Modave<sup>2</sup>, and Lionel Pichon<sup>1</sup>

<sup>1</sup>Laboratoire de Genie Electrique de Paris, UMR 8507 CNRS, SUPELEC, Université Paris Sud et Université Pierre et Marie Curie, Plateau du Moulon, 91192 Gif sur Yvette cedex, France

<sup>2</sup>Université de Liège, Department of Electrical Engineering and Computer Science, Montefiore institute Liège 4000, Belgique

**This paper presents a modeling of thin sheets. An interface condition based on analytical solution is used to avoid a fine mesh. This condition is integrated in a time domain Discontinuous Galerkin method in order to evaluate the shielding effectiveness. This approach is validated by a comparison with analytical solution. 2D and 3D cavities are simulated to illustrate the efficiency of the condition.**

*Index Terms*—Electromagnetic compatibility, Discontinuous Galerkin methods, thin sheet, interface condition.

## I. INTRODUCTION

**M**ANY problems in electromagnetic compatibility (EMC) require adequate numerical approaches to evaluate shielding effectiveness. The ability to model features that are small relative to the cell size is often important in electromagnetic simulations. This may lead to subsequent increase in memory and execution time due to a refined mesh around small details of the geometry. Also the quality of the mesh can be strongly affected. The impact of thin sheets is even more so consequent for the time domain computations.

In order to avoid the spatial discretization of thin sheets different interface conditions have been proposed. In the frequency domain, interface condition is developed using analytical solutions [1]. This condition can be included in a three dimensional model [2]. In the time domain, an inverse Fourier or Laplace transform is combined to a convolution product. Many papers have been devoted to implement this approach in the FDTD method [3][4][5]. Nevertheless the stair casing error present in the FDTD method may affect significantly the numerical results.

The Discontinuous Galerkin (DG) method is a powerful approach for solving time dependent problems [6]. It is based on the local solution of the equations in each cell and uses flux terms to connect adjacent elements. It has the advantage of the unstructured mesh and high spatial order scheme unlike the conventional FDTD. Such a high spatial scheme can reduce the dispersive error induced by the low level of the spatial approximation in the FDTD.

In this paper a sheet interface condition is built to replace a thin sheet. A general time domain formulation is proposed to take into account the physical characteristics of the sheet. The approach is based on rational approximation and a recursive algorithm to compute the convolution products. For low frequencies (when the skin depth is larger than the thickness)

a simplified expression is derived.

This interface condition is implemented in a DG module of GMSH [7].

## II. PROBLEM FORMULATION

Maxwell's equation are solved in the time domain:

$$\begin{cases} \epsilon \partial_t \vec{E} - \nabla \times \vec{H} &= -\vec{J} \\ \mu \partial_t \vec{H} + \nabla \times \vec{E} &= 0 \end{cases} \quad (1)$$

where  $\epsilon$  is the permittivity of the medium and  $\mu$  its permeability. The current density of the conductive medium is such as  $\vec{J} = \sigma \vec{E}$ , with  $\sigma$  the conductivity.

The DG variational formulation of (1) in each element  $T$  is given by[6]:

$$\begin{cases} \int_T \epsilon \partial_t \vec{E} \cdot \vec{\phi} - \int_T \vec{H} \cdot \nabla \times \vec{\phi} - \int_{\partial T} (\vec{n} \times \vec{H})^{num} \cdot \vec{\phi} = - \int_T \sigma \vec{E} \cdot \vec{\phi} \\ \int_T \mu \partial_t \vec{H} \cdot \vec{\psi} + \int_T \vec{E} \cdot \nabla \times \vec{\psi} + \int_{\partial T} (\vec{n} \times \vec{E})^{num} \cdot \vec{\psi} = 0 \end{cases} \quad (2)$$

where  $\vec{\phi}$  and  $\vec{\psi}$  are test functions.

The interface terms between adjacent elements are evaluated using numerical fluxes  $(\vec{n} \times \vec{E})^{num}$  and  $(\vec{n} \times \vec{H})^{num}$  given by[6]:

$$\begin{cases} (\vec{n} \times \vec{H})^{num} &= \vec{n} \times \frac{\{Z\vec{H}\}}{\{Z\}} - \alpha (\vec{n} \times \frac{(\vec{n} \times \{\vec{E}\})}{\{Z\}}) \\ (\vec{n} \times \vec{E})^{num} &= \vec{n} \times \frac{\{Y\vec{E}\}}{\{Y\}} + \alpha (\vec{n} \times \frac{(\vec{n} \times \{\vec{H}\})}{\{Y\}}) \end{cases} \quad (3)$$

where  $Z = \frac{1}{Y} = \sqrt{\frac{\mu}{\epsilon}}$ ,  $[u] = \frac{u^+ - u^-}{2}$  and  $\{u\} = \frac{u^+ + u^-}{2}$ .

The “-” denotes the values in the current element, and “+” for the adjacent element. For  $\alpha = 0$ , centred fluxes are obtained and the numerical scheme is only dispersive [8]. For  $\alpha = 1$ , upwind fluxes are obtained and the numerical scheme is additionally dissipative [6].

For simulations, an implicit second order Runge-Kutta scheme that permits a large time step is considered for time

discretization, and a first spatial order with upwind fluxes is used for the spatial scheme.

### III. CONSTRUCTION OF THE INTERFACE CONDITION

The electromagnetic field equations in the sheet are considered in 1D and in the frequency domain[1]:

$$\begin{cases} \partial_x E_y = -j\omega\mu H_z \\ \partial_x H_z = -(\sigma + j\omega\epsilon)E_y \end{cases} \quad (4)$$

where  $\epsilon$ ,  $\mu$  and  $\sigma$  are respectively the permittivity, the permeability and the conductivity of the sheet (Fig. 1), its thickness is  $d$ .

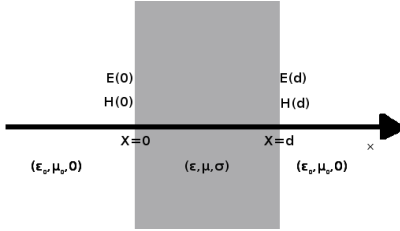


Figure 1: Geometry of the thin sheet

Using the analytical 1D solution of (4), the electromagnetic fields on the both sides of the sheet are connected by:

$$\begin{pmatrix} E_y(\omega, d) \\ H_z(\omega, d) \end{pmatrix} = \begin{pmatrix} \cosh(\gamma d) & \eta \sinh(\gamma d) \\ \eta^{-1} \sinh(\gamma d) & \cosh(\gamma d) \end{pmatrix} \begin{pmatrix} E_y(\omega, 0) \\ H_z(\omega, 0) \end{pmatrix} \quad (5)$$

where  $\gamma$  the planar propagation constant:

$$\gamma = \sqrt{\mu\omega(j\sigma - \epsilon\omega)} \quad (6)$$

and  $\eta$  is the intrinsic impedance of the sheet:

$$\eta = \sqrt{\frac{\mu\omega}{\epsilon\omega - j\sigma}} \quad (7)$$

This relation can be rewritten as an impedance relation for a layer:

$$\begin{pmatrix} E_y(\omega, 0) \\ E_y(\omega, d) \end{pmatrix} = \begin{pmatrix} \hat{z}_1(\omega) & -\hat{z}_2(\omega) \\ \hat{z}_2(\omega) & -\hat{z}_1(\omega) \end{pmatrix} \begin{pmatrix} H_z(\omega, 0) \\ H_z(\omega, d) \end{pmatrix} \quad (8)$$

whith:

$$\begin{cases} \hat{z}_1(\omega) = -\frac{\eta}{\tanh(\gamma d)} \\ \hat{z}_2(\omega) = -\frac{\eta}{\sinh(\gamma d)} \end{cases} \quad (9)$$

The time domain relation of (8) is a convolution product:

$$\begin{pmatrix} E_y(t, 0) \\ E_y(t, d) \end{pmatrix} = \begin{pmatrix} z_1(t) & -z_2(t) \\ z_2(t) & -z_1(t) \end{pmatrix} * \begin{pmatrix} H_z(t, 0) \\ H_z(t, d) \end{pmatrix} \quad (10)$$

where  $z_1$  and  $z_2$  are respectively the Inverse Fourier Transform (IFT) of  $\hat{z}_1$  and  $\hat{z}_2$ .

Let note  $(\vec{E}^0, \vec{H}^0)$  and  $(\vec{E}^d, \vec{H}^d)$  the fields on the sides of the sheet and  $\vec{n}$  the outward unit normal. The relation (10) can be reformulated with tangential components of the fields in the general case and becomes:

$$\begin{cases} \vec{n} \times \vec{E}^0(t) = \vec{n} \times [\vec{n} \times (z_1 * \vec{H}^0(t) - z_2 * \vec{H}^d(t))] \\ \vec{n} \times \vec{E}^d(t) = \vec{n} \times [\vec{n} \times (z_2 * \vec{H}^0(t) - z_1 * \vec{H}^d(t))] \end{cases} \quad (11)$$

## IV. IMPLEMENTATION OF THE SHEET CONDITION

### A. General sheet condition

The implementation of the relation (11) is performed in two steps, the first step consists to compute the IFT of the impedance functions  $\hat{z}_1$  and  $\hat{z}_2$ . The second step consists in computing the convolution production between the impedance functions and the magnetic fields.

The impedance functions  $\hat{z}_1$  and  $\hat{z}_2$  are characterized by a wide band spectrum. Evaluation of their discrete IFT has a significant time cost and sometimes the results are not very accurate. The equivalent rational approximations are considered in the frequency domain using the Vector Fitting procedure [9].

The rational approximations of the impedance functions defined in (9) are:

$$\begin{cases} \hat{z}_1(\omega) = z_{1,0} + \sum_{k=1}^{N_1} \frac{R_{1,k}}{j\omega - p_{1,k}} \\ \hat{z}_2(\omega) = z_{2,0} + \sum_{k=1}^{N_2} \frac{R_{2,k}}{j\omega - p_{2,k}} \end{cases} \quad (12)$$

where  $z_{i,0}$  are the asymptotic high-frequency value of  $\hat{z}_i(\omega)$ ,  $R_{i,k}$  is the  $k$ th residue,  $p_{i,k}$  is the  $k$ th pole, and  $N_i$  the number of poles of the rational approximation.

The IFT is calculated analytically from the rational approximation, the transient impedance functions are:

$$\begin{cases} z_1(t) = z_{1,0}\delta(t) + \sum_{k=1}^{N_1} R_{1,k} \exp(p_{1,k}t) \\ z_2(t) = z_{2,0}\delta(t) + \sum_{k=1}^{N_2} R_{2,k} \exp(p_{2,k}t) \end{cases} \quad (13)$$

The convolution integrals are determined numerically using the piecewise linear recursive formulation proposed in [10]. The numerical formulation of the relation (11) for the  $m$ th time iteration is written as:

$$\begin{cases} \vec{n} \times \vec{E}^{0,m} = \vec{n} \times [\vec{n} \times (\vec{E}_1^{0,m} - \vec{E}_2^{d,m})] \\ \vec{n} \times \vec{E}^{d,m} = \vec{n} \times [\vec{n} \times (\vec{E}_2^{0,m} - \vec{E}_1^{d,m})] \end{cases} \quad (14)$$

with

$$\begin{cases} \vec{E}_i^{j,m} = z_{i,0} \vec{H}^{j,m} + \sum_{k=1}^{N_i} \frac{\vec{z}_{i,k}^{j,m}}{\zeta_{i,k}^{j,m}} \\ \zeta_{i,k}^{j,m} = q_{1,k} \zeta_{i,k}^{j,m-1} + q_{2,k} \vec{H}^{j,m-1} + q_{3,k} \vec{H}^{j,m} \\ q_{1,k} = \exp(\beta_k) \\ q_{2,k} = \frac{\alpha_k}{\beta_k} [1 + (\beta_k - 1) \exp(\beta_k)] \\ q_{3,k} = \frac{\alpha_k}{\beta_k} [\exp(\beta_k) - \beta_k - 1] \\ \alpha_k = \frac{R_{i,k}}{p_{i,k}} \\ \beta_k = p_{i,k} \Delta t \end{cases} \quad (15)$$

for  $j \in \{-, +\}$ ,  $i \in \{1, 2\}$ ,  $k \in \{1, 2, \dots, N_i\}$  and the time step  $\Delta t$ .

For an interface representing the sheet, let consider  $(\vec{E}^-, \vec{H}^-) = (\vec{E}^0, \vec{H}^0)$  the fields for the current element “-”, and  $(\vec{E}^+, \vec{H}^+) = (\vec{E}^d, \vec{H}^d)$  the fields for the adjacent element “+”. The resulting flux terms for the current element for this interface are obtained by taking only the magnetic field for

the current element, and the electric field is taken from the second expression of the relation (14).

$$\begin{cases} (\vec{n} \times \vec{H})^{num,n} = \vec{n} \times \vec{H}^{-,n} \\ (\vec{n} \times \vec{E})^{num,n} = \vec{n} \times \vec{E}^{+,n} \end{cases} \quad (16)$$

### B. Simplified sheet condition

For the low frequencies, the electric fields are supposed constant inside the sheet, and  $\epsilon\omega \ll \sigma$ .

When  $\omega \rightarrow 0$ ,  $\omega\epsilon$  can be neglected. The impedance and the propagation constant can be rewritten:

$$\begin{cases} \eta = \sqrt{\frac{j\omega\mu}{\sigma}} \\ \gamma = \sqrt{j\omega\mu\sigma} \end{cases} \quad (17)$$

The asymptotic behaviour of  $(\hat{z}_1 + \hat{z}_2)$  is:

$$(\hat{z}_1 + \hat{z}_2) = -\frac{2}{\sigma d} \quad (18)$$

The relation (10) is rewritten by using the average of the electric field:

$$\begin{cases} \vec{E}^d(\omega) = \vec{E}^0(\omega) \\ \frac{\vec{E}^d(\omega) + \vec{E}^0(\omega)}{2} = \frac{1}{2}(\hat{z}_1 + \hat{z}_2) * (\vec{H}^0 - \vec{H}^d) \end{cases} \quad (19)$$

A simple form of (11) is obtained by supposing the average of the electric fields on the sides of the sheet:

$$\begin{cases} \vec{n} \times \vec{E}^0(t) = \frac{1}{\sigma d} \vec{n} \times [\vec{n} \times (\vec{H}^d(t) - \vec{H}^0(t))] \\ \vec{n} \times \vec{E}^d(t) = \frac{1}{\sigma d} \vec{n} \times [\vec{n} \times (\vec{H}^d(t) - \vec{H}^0(t))] \end{cases} \quad (20)$$

The resulting flux terms for this simplified sheet condition are:

$$\begin{cases} (\vec{n} \times \vec{H})^{num} = \vec{n} \times \vec{H}^- \\ (\vec{n} \times \vec{E})^{num} = \frac{1}{\sigma d} \vec{n} \times \vec{n} \times (\vec{H}^+ - \vec{H}^-) \end{cases} \quad (21)$$

These flux terms are independent of the recursive procedure, and are the same complexity as an ordinary flux terms. This condition is valid when the thickness of the sheet is smaller than the skin depth.

## V. NUMERICAL RESULTS

### A. 1D Validation Test

To validate the general sheet condition,  $\vec{E} = (0, 0, E_z)$ ,  $\vec{H} = (0, H_y, 0)$ , and two vacuum mediums separated by a conducting sheet are considered. The permittivity, the permeability, the conductivity and the thickness of this sheet are respectively  $\epsilon = 5\epsilon_0$ ,  $\mu = 5\mu_0$ ,  $\sigma = 2000 S/m$  and  $d = 1 mm$ , where  $\epsilon_0$  and  $\mu_0$  are the permittivity and the permeability of the vacuum medium (Fig.1). This sheet is illuminated by an harmonic plane wave for different frequencies. The skin depth varies between 1 mm and 0.22 mm. Let note  $\vec{E}_i$ ,  $\vec{E}_t$  the incident and the transmitted electric fields. The Shielding Effectiveness for the electric field ( $SE_E$ ) is defined by the following expression:

$$SE_E = 20 \log_{10} \left( \frac{|\vec{E}_i|}{|\vec{E}_t|} \right) \quad (22)$$

Fig.2 illustrates the comparison of the  $SE_E$  between the solution computed with the general sheet condition and the

analytical solution calculated in the frequency domain. The transmitted electric field is taken in the harmonic regime to calculate  $SE_E$ . The difference is negligible.

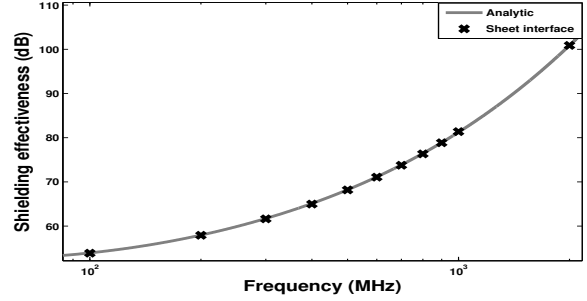


Figure 2: Shielding Effectiveness

The same sheet is illuminated by an incident Gaussian pulse. The minimum of the skin depth is 0.3 mm. The computed solution using the general sheet interface is compared to the solution obtained when the sheet is meshed in Fig.3. The difference is also negligible and demonstrates that the transient regime is also taken account.

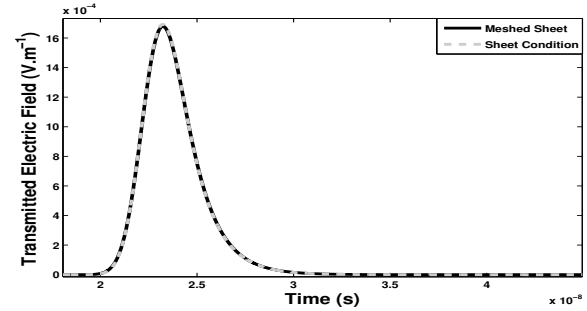


Figure 3: Transient Transmitted Field

This condition is also valid for low conductivities, even if the wavelength is smaller than de skin depth. For  $\sigma = 10^{-4} S/m$ , the error of the transmitted electric field between analytical and computed solution remains less than 1%.

These examples validate the sheet condition for the general case.

### B. 2D cavity

Let consider 50 cm x 40 cm cavity. A 10 cm aperture is located on the front side. The characteristics of the walls are  $\epsilon = \epsilon_0$ ,  $\mu = \mu_0$ ,  $\sigma = 50 S/m$  and  $d = 1 mm$  (Fig.4). This cavity is illuminated by the Gaussian pulse used in the 1D example. The incident field is normal to the aperture. This pulse excites the frequencies up to 1GHz and the minimum of the skin depth is 4.5 mm.

The solution is computed for two cases. The first case using the simplified sheet condition and the second when the sheet is meshed. For the first case 3000 elements are used. For the second case 13000 elements are used with 10000 elements only for the walls of 1 mm thickness. A personal computer 3.05 GHz Pentium are used. The time cost of simulation is 4 hours for the first case and 20 hours for the second.

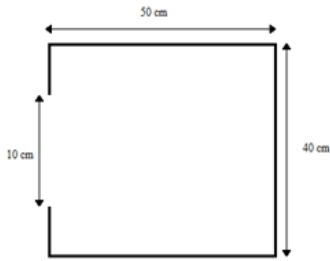


Figure 4: 2D cavity

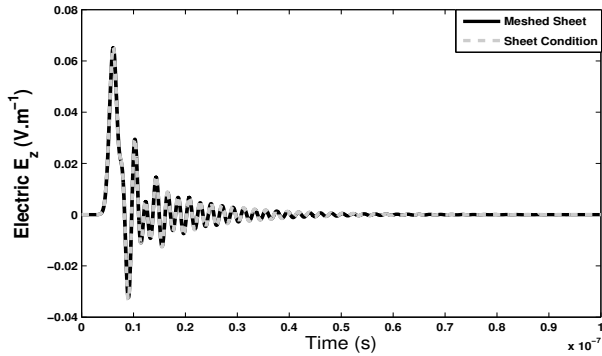


Figure 5: Electric field at the center of the cavity in the time domain

In Fig.5, the electric field in the center of the cavity is shown. This example illustrates the efficiency of the condition for problems with thin conductive walls.

### C. 3D cavity

A transient scattering problem is studied. Let consider a 3D cavity (Fig. 6)[11], whose dimensions are  $a = 300 \text{ mm}$ ,  $b = 120 \text{ mm}$ ,  $d = 300 \text{ mm}$ ,  $l = 100 \text{ mm}$ ,  $w = 5 \text{ mm}$ ,  $t = 1 \text{ mm}$ .

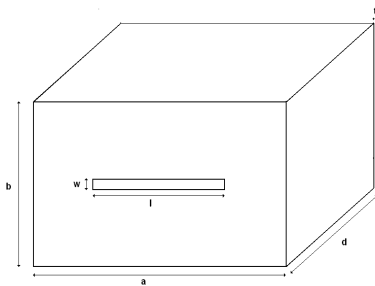


Figure 6: 3D Cavity

This cavity is illuminated by the previous incident Gaussian pulse. Different cases of conductivity of the walls are compared:  $\sigma = 200 \text{ S/m}$ ,  $\sigma = 50 \text{ S/m}$  and Perfect Electric Conductor (PEC). For finite conductivities, the simplified sheet condition is used. A Fast Fourier transform is applied to the electric field in the center of the cavity, and the shielding effectiveness is plotted in Fig.7. The result obtained for the

PEC case is similar to the analytical formulation [11]. For the finite conductivities, the shielding effectiveness is lower and the resonance peaks are attenuated.

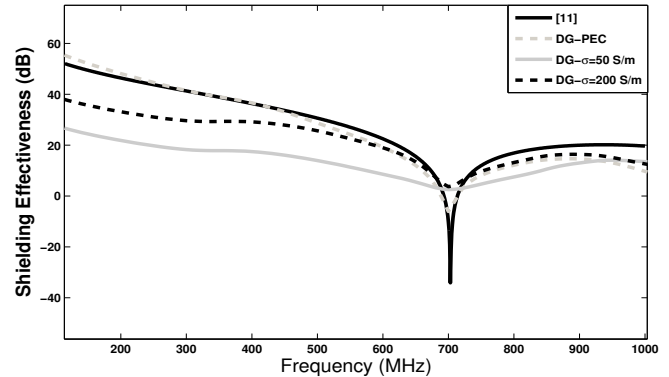


Figure 7: Shielding effectiveness of the electric field in the center of the cavity in the frequency domain

## VI. CONCLUSION

An interface condition to avoid the mesh of thin sheets is presented. It allows a reduction of the computational time cost. The interface condition is implemented in a 3D time domain Discontinuous Galerkin Method and is validated. The future developments will extend the interface condition for the case of multilayer and heterogeneous material.

## REFERENCES

- [1] K. M. Mitzner, "Effective Boundary Conditions for Reflection and Transmission by an Absorbing Shell of Arbitrary Shape," *IEEE Trans. Anten. and Propag.*, vol.16, no.6, pp. 706-712, 1968.
- [2] F. Bocquet, L. Pichon, A. Razek, "3D FEM Analysis of Electromagnetic Wave Scattering from a Dielectric Sheet in EMC Problems," *IEEE Trans. on Magnetics*, vol.34, no.5, pp. 2791-2794, 1998.
- [3] M.S. Sarto, "A new Model for the FDTD Analysis of the Shielding Performances of Thin Composite Structures," *IEEE Trans. Electromagnetic Comp.*, vol.41, no.4, pp. 298-306, 1999.
- [4] M. Feliziani, F. Maradei, G. Tribellini, "Field Analysis of Penetrable Conductive Shields by The Finite-Difference Time-Domain Method with Impedance Network Boundary Conditions (INBCs)," *IEEE Trans. Electromagnetic Comp.*, vol.41, no.4, pp. 307-319, 1999.
- [5] M. Feliziani, "Subcell FDTD Modeling of Field Penetration Through Lossy Shields," *IEEE Trans. Electromagnetic Comp.*, vol.54, no.2, pp. 299-307, 2012.
- [6] J. S. Hesthaven, T. Warburton, "Nodal High-Order Methods on Unstructured Grids," *Journal of Computational Physics*, vol.181, pp. 186-221, 2002.
- [7] C. Geuzaine, J.-F. Remacle, "Gmsh: a Three-Dimensional Finite Element Mesh Generator with Built-in Pre- and Post-Processing Facilities," *International Journal for Numerical Methods in Engineering*, vol.77, no.11, pp. 1309-1331, 2009.
- [8] L. Fezoui, S. Lanteri, S. Lohrengel, S. Piperno, "Convergence and Stability of a Discontinuous Galerkin Time-Domain Method for the 3D Heterogeneous Maxwell Equations on Unstructured Meshes," *M2AN*, vol.39, no.6, pp. 1149-1176, 2005.
- [9] B. Gustavsen, A. Semlyen, "Rational Approximation of Frequency Domain Response by Vector Fitting," *IEEE Power Eng. Soc. Winter Meet.*, Tampa, FL, Feb. 1998, PE-194-PWRD-0-117.
- [10] K. S. Oh, J. E. Shutt-Aine, "An Efficient Implementation of Surface Impedance Boundary Condition for the Finite-Difference Time Domain Method," *IEEE Trans. Antennas Propagat.*, vol.43, no.7, pp. 660-666, 1995.
- [11] M. P. Robinson, T.M. Benson, C. Christopoulos, J. F. Dawson, M. D. Ganley, A. C. Marvin, S. J. Porter, D. W. P. Thomas, "Analytical Formulation for the Shielding Effectiveness of Enclosures with Apertures," *IEEE Trans. Electromagnetic Comp.*, vol.40, no.3, pp. 240-248, 1998.